

NANO EXPRESS

Open Access



Influence of Water on the Structure and Dielectric Properties of the Microcrystalline and Nano-Cellulose

Kostiantyn M. Kovalov*, Olexander M. Alekseev, Maxim M. Lazarenko, Yu F. Zabashta, Yurii E. Grabovskii and Sergii Yu Tkachov

Abstract

Influence of water in the different states on a structure and dielectric properties of microcrystalline cellulose were studied by of X-ray, thermogravimetry, and dielectric spectroscopy. At research of microcrystalline cellulose (MCC) with different content of water, it is shown that the molecules of water are located in the macropores of MCC and in multimolecular hydrated layers. It is shown that at the increase of concentration of water in a hydrated shell, the reorganization of molecules of cellulose in the surface of crystallites takes place, and as a result, their transversal size and crystallinity increase. It is shown that during the concentration of water, more than 13% in a continuous hydrated shell of crystallites appears. Temperature dependences of actual and imaginary parts of complex dielectric permittivity were studied in the interval of temperatures $[-180 \div 120]$ °C on frequencies of $f = 5, 10, 20,$ and 50 kHz. A low-temperature relaxation process and high-temperature transition were observed. Low-temperature relaxation process which is related to transition of surface methylol groups of molecules of cellulose conformation from *tg* to *tt* is shifted toward low temperatures at the increase of concentration of water in microcrystalline cellulose.

Keywords: Microcrystalline cellulose, Relaxation, X-ray, Dielectric permittivity

Background

Usual cellulose from various vegetative sources, which is practically inexhaustible renewable ecologically clean resource, is a raw material for production of microcrystalline cellulose (MCC). It determines the growing interest for investigation of its physical and physicochemical properties. Another important factor, which attracts attention of investigators, is availability of the crystalline particles in the MCC structure, the study of properties of which is promising for many directions of development of modern technologies. The most developed from such directions are pharmaceutical industry and cosmetics [1]; however, currently, MCC begins to be used as a filler in composite materials [2], modern electronics [3], and laser optics [4, 5]. In this regard, the ability of MCC to absorb moisture, which can substantially affect on its properties, in particular, structural [6], electrical [7, 8], and thermophysical [9, 10] ones, is important.

Methods

The Samples

The samples of MCC (Cellets-100) grade, produced by Shin-Etsu Company (Japan), were used for investigation. Initial MCC was dispersed in an agate mortar. To obtain water-free samples, the samples were held in the drying box during 3 days at the temperature of 115 °C, and then, they were encapsulated in the vacuum press mold. The samples with different level of moisture were obtained by their holding during different times in under saturated water vapor.

Equipment

Analysis of the sample structure was performed using X-ray diffractometer DRON-3M with the tube BSV-28 ($\lambda = 1.54178$ Å).

Differential thermal analysis (DTA) and thermogravimetric investigations were performed using derivatograph Q-1500D. Investigations were carried out within the temperature range $T = 20 \div 250^\circ$ with the rate of 5 °C/min.

* Correspondence: kovalovkostya@univ.kiev.ua
Taras Shevchenko National University of Kyiv, Volodymyrska str. 64/13, Kyiv 01601, Ukraine

The samples for dielectric investigations were produced by the compacting of MCC powder between coatings from a stainless steel at the pressure of 120 kg/cm². Then, the sample with laminated coatings was placed in the thermostabilized four-electrode cell, which permitted to control the sample thickness during measurements using an additional air-dielectric capacitor. Measurements of the capacity and loss factor of this cell on four different frequencies $f = 5, 10, 20, 50$ kHz within the temperature range $(-180 \div 120)$ °C were performed using automated installation based on the alternating current bridge P5083 [11].

Results and Discussion

Thermogravimetric Investigations

Investigations of the amount of water in MCC were performed using derivatograph Q-1500D. In the investigated sample, the temperature (T), mass change (m), and rate of the mass change (dm/dT) were measured simultaneously and differential and thermal analyses (DTA) were performed.

Temperature dependencies of the relative mass change $\Delta m/m_0 = (m - m_0)/m_0$, m_0 —initial sample mass (see Fig. 1) and derivative of the mass change dm/dT (see Fig. 2) were obtained.

One can consider that the loss of mass by the sample is caused by the evaporation of water, which is located in the sample in different states [12, 13]. Therefore, the dm/dT was divided on peaks using the Gauss distribution (see Fig. 3).

The dependence of dm/dT for each of the investigated samples can be described by the superposition of three peaks. The first peak (f_1) is connected with the evaporation of water of physical-mechanical bond with MCC, which is located in the micropores of the sample, the

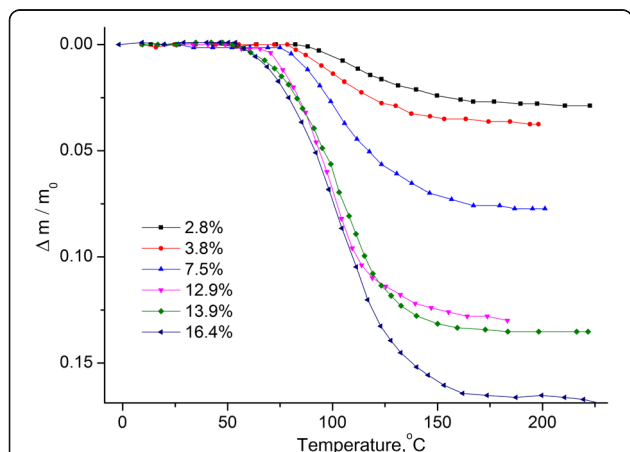


Fig. 1 Temperature dependence of the relative mass change of MCC. Temperature dependence of the relative mass change $\Delta m/m_0$ of MCC samples with different water content

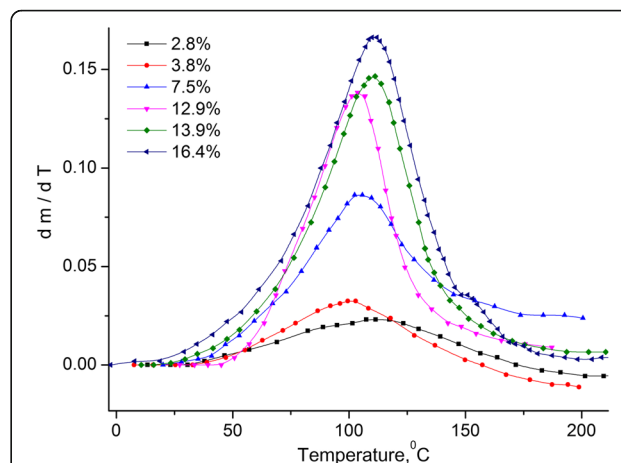


Fig. 2 Temperature dependence of the derivative of mass change of MCC. Temperature dependence of the derivative of mass change dm/dT of MCC samples with different water content

second one (f_2) is caused by the water of polymolecular and monomolecular hydrate layers, and the third peak is caused by the thermal oxidative degradation of the sample.

In Table 1, percentage S_1 in the square of the general peak dm/dT and mass percentage $w_i = CS_i/100\%$ into general mass of different types of water and destruction for the MCC samples with different water content is shown.

It is seen that the amount of physically mechanically bound water S_1 increases with the growth of the content of general water, and the amount of water in hydrate shells S_2 also increases and reaches its saturation at concentration of the general water of 12.9%.

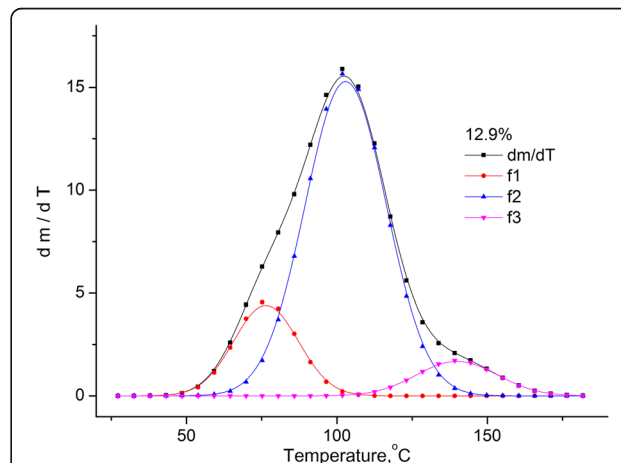


Fig. 3 Approximation of the dm/dT dependence for MCC sample with the humidity of 12.9%. Approximation of the dm/dT dependence for MCC sample with the humidity of 12.9% using Gauss distribution with three peaks

Table 1 Contributions of different types of water and destruction for the MCC samples with different water content in the square of the general peak on the graph dm/dT and its content in the samples

C (general water content in MCC), %	I (f_1) $S_1, \%$	I (f_1) $W_1, \%$	II (f_2) $S_2, \%$	II (f_2) $W_2, \%$	III (f_3) $S_3, \%$	III (f_3) $W_3, \%$
2.8	–	–	100	2.8	–	–
3.8	3.3	0.1	88.7	3.4	7.9	0.3
7.5	7.1	0.5	84.3	6	8.5	0.6
12.9	15	1.9	77	10	7.5	1
13.9	21	3.1	72	10	6	0.8
16.4	26	4	67	10.7	6.8	1

Let us consider in more details the second peak (f_2), which is caused by cellulose crystals dehydration.

The method for calculation of kinetic parameters of the dehydration process, such as the energy of activation E and pre-exponential factor (k_0) are described in [12]. Kinetic equation of the desorption process may be presented as:

$$\frac{dQ}{dt} = -kQ^n, k = \frac{-dQ/dt}{Q^n}. \tag{1}$$

A degree of covering of cellulose crystallites by the water molecules (Q) changes from 1 (for initial material) to 0 (whole water is dehydrated). An order of reaction (n) is an integer from 1 to 3; it is assumed that it is known from the experiment. The constant of the reaction rate (k) can be written as:

$$k = k_0 \exp\left(-\frac{E}{RT}\right), \tag{2}$$

where R is universal gas constant. The value of E is taken in this approximation as a constant, which means an equivalence of all hydration centers of the MCC crystals surface. The pre-exponential factor can be written as $k_0 = ZP$, where Z is the theoretical number of discontinuities of hydrogen bonds between water molecules and cellulose (MCC) in a hydrate layer per unit time, and P is a probability factor that takes into account all the effects caused by a deviation from ideality. The probability of breaking the hydrogen bond between the water molecule and the cellulose is much greater at a higher concentration of water molecules in the hydrated shell, so the water molecule after the bond break does not form a new bond with the neighboring free node, but translates from the hydrate layer. Therefore, the pre-exponential factor of the reaction rate is small at the low concentrations of water and increases with the growth of water concentration in the hydrated shell. When saturation of the hydrated shell is achieved (all nodes are occupied),

then k_0 does not depend on the concentration of the moisture. This is observed for the MCC water system at a concentration more than 12.9%.

After substitution of Eq. 1 in Eq. 2 and logarithmation, we obtain:

$$\ln k = \ln\left[\frac{-dQ/dt}{Q^n}\right] = \ln k_0 - \frac{E}{RT}. \tag{3}$$

Under initial conditions $Q_{t=0} = 1$, $Q_{t=\infty} = 0$ and constant heating rate (β), i.e., at linear dependence of the temperature on time

$$T(t) = T_0 + \beta t, \tag{4}$$

the following relationships are fulfilled

$$Q(t) = \frac{S_T}{S_0}; -\frac{dQ}{dt} = \beta \frac{f_3}{S_0}, \tag{5}$$

where S_0 and S_T are the areas on the plot f_2 under the whole peak and the part of the peak from T to ∞

$$S_T = \int_T^\infty f_2 dT, S_0 = \int_0^\infty f_2 dT. \tag{6}$$

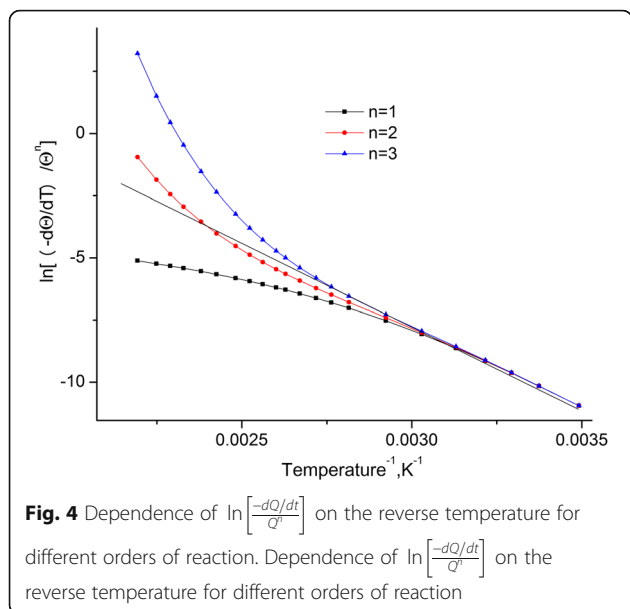
If all assumptions, which are placed in this method are correct and the order of reaction n is chosen correctly, then the dependence $\ln\left[\frac{-dQ/dt}{Q^n}\right]$ on the inverse temperature (Eq. 3) is linear in the whole temperature range. Having experimental values of f_3 and β , using expressions Eqs. 5 and 6, one can obtain Q and dQ/dt , and parameters of non-isothermal kinetics k_0 and E are calculated from Eq. 3.

An advantage of this method is the usage of the whole array of experimental data, including high temperature part of the thermogram, which is especially important at determination of the order n , determination of the reaction mechanism, and model fairness.

The dependences of $\ln\left[\frac{-dQ/dt}{Q^n}\right]$ from a reverse temperature for the investigated standards (Fig. 4) were built. These dependences are approximated by straight lines by means of least-squares method. It is found out that the highest coefficient of Pearson is observed at $n = 2$.

Calculated activation energy (E) and pre-exponential factor (k_0) of the investigated MCC samples are presented in Table 2 (see Fig. 5). Assuming that the activation energy is connected with the rupture of the hydrogen bonds, which comprise 25 kJ/mol [10], it is possible to calculate their number N_I (see Table 2).

It is seen that with the growth of concentration of physically and chemically bound water, the increase of activation energy (E) is observed, and at concentration



of 12.9%, it reaches its saturation. The value of activation energy for the saturated state corresponds to eight hydrogen bonds.

Therefore, we can assume that at water concentration of 12.9%, the continuous hydrate shell of MCC crystals is formed in the sample.

X-ray Diffraction Analysis

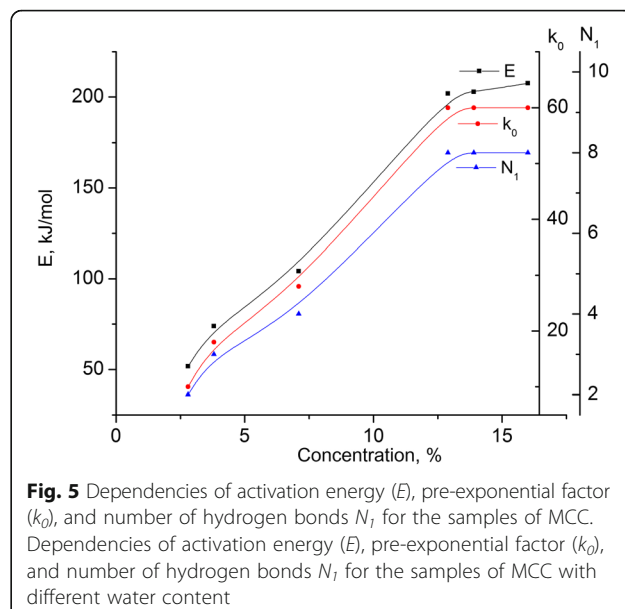
The dependencies of diffracted X-ray radiation intensity for microcrystal cellulose with different water concentrations on diffraction angle $I(2\theta)$ within the angles range $[5 \div 45]^\circ$ (see Fig. 6) with the step of angle change 0.1° were obtained.

Maxima, which correspond to different crystallographic plains, are observed on the MCC X-ray diffractogram (see Fig. 6).

The degree of crystallinity (C_k) of MCC was calculated by the integral intensity of X-rays scattering as a ratio of structural reflexes to total intensity of the diffraction pattern excluding background in the range $2\theta [5 \div 45]^\circ$ (see Fig. 6). Data of C_k for MCC samples are presented in Table 3 [14].

Table 2 Dependencies of activation energy (E), pre-exponential factor (k_0), and number of hydrogen bonds N_1 on water content in the investigated samples

C (water content in MCC), %	k_0	E , kJ/mol	N_1
2.8	10	51.75	2
3.8	18	73.92	3
7.1	28	104.19	4
12.9	60	201.91	8
13.9	60	202.82	8
16.4	60	207.58	8



Transverse dimensions of cellulose crystallites in normal direction to the system were calculated by Debye–Sherrer formula [15].

$$B_{hkl} = \frac{k\lambda}{h \cdot \cos\theta_{hkl}}, \tag{7}$$

where $k = 0.94$ —dimensionless form-factor, λ —wavelength of $\text{CuK}\alpha$ -radiation (1.54178 \AA); h —half-width of (hkl) reflex, θ_{hkl} —angle of diffraction from the (hkl) plains system. Urotropine was used as an etalon for higher confidence. Instrumental error was estimated using the etalon, and corrections for the reflex half-width were calculated.

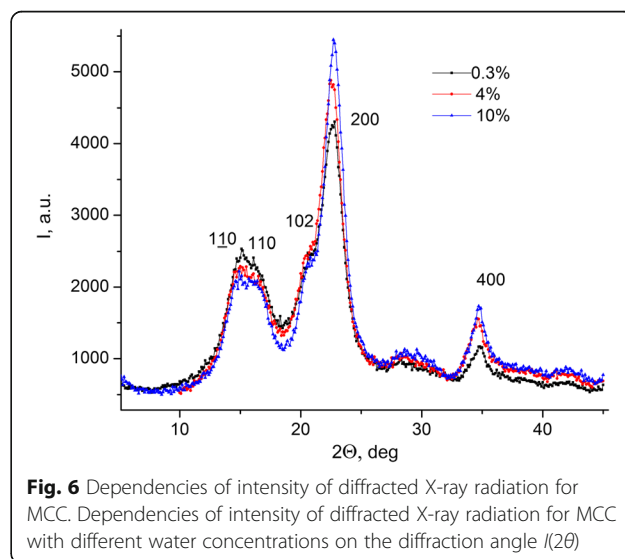


Table 3 Transversal dimensions of crystallites B_{hkl} and degree of crystallinity C_k for the samples of MCC with different content of water

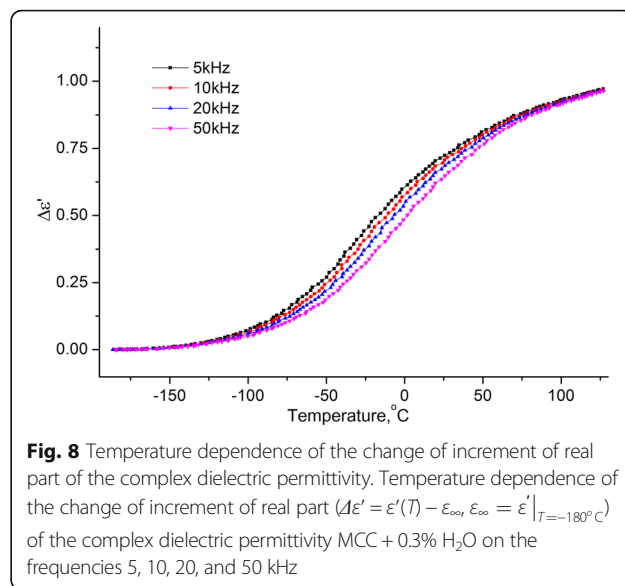
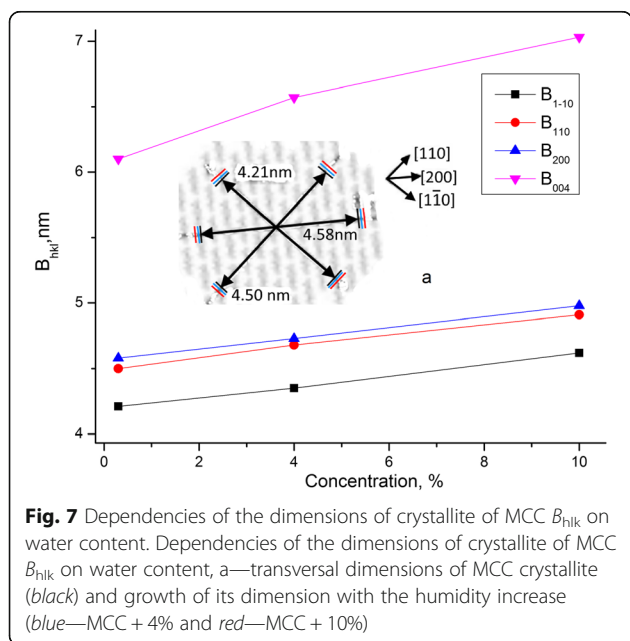
C (water content in MCC), %	0.3	4	10
B_{110} , nm	4.21	4.35	4.62
B_{110r} , nm	4.50	4.68	4.91
B_{102r} , nm	5.98	6.14	6.37
B_{200r} , nm	4.58	4.73	4.98
B_{004r} , nm	6.1	6.57	7.03
C_k , %	58	65	68

Data of dimensions B_{hkl} for MCC samples with different water content and crystallinity are presented in Table 3.

It follows from the obtained results (Table 3 and Fig. 7) that transversal dimension of crystallites and crystallinity grow with water concentration. Growth of dimensions takes place by different directions on approximately 0.4 nm. Average diameter of cellulose molecule is of an order of $d = 0.8$ nm. Therefore, with the growth of water concentration, an ordering of cellulose molecules in the boundary layer may happen, and, as a consequence, increase of transversal dimension of cellulose crystallites and crystallinity can take place.

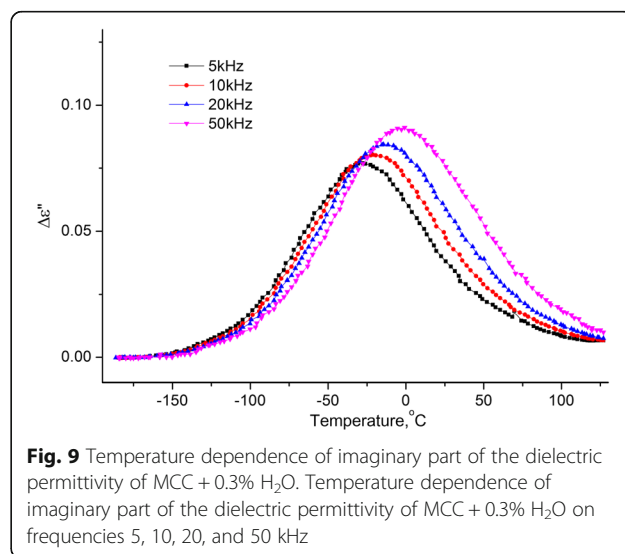
Dielectric Properties of MCC

Temperature dependencies of the real and imaginary parts of the complex dielectric permittivity within the temperature range $[-180 \div 120]$ °C on the frequencies $f = 5, 10, 20,$ and 50 kHz for the samples MCC + 0.3% H₂O (see Figs. 8 and 9) were investigated.



From the two processes observed on the temperature dependences of $\Delta\epsilon'(T)$ and $\epsilon''(T)$, the low temperature is a relaxation since the maximum on $\Delta\epsilon'(T)$ and the inflection on $\epsilon''(T)$ is shifted with the increasing of the frequency. Usually, this process is called the β -process, its molecular mechanism is not finally established. We assume that it is related to the reorientation of methylol groups on the surface of the crystallites of the MCC, and this reorientation occurs with a change in the conformation of the methylol groups tg to tt , the breakup of the intra-molecular H bond and the formation of the H bond with the adsorbed water molecule [16].

The high-temperature process on the dependences $\Delta\epsilon'(T)$ and $\epsilon''(T)$ does not shift with the frequency variation, its intensity grows with the concentration of the



water in the MCC (see Figs. 10 and 11). We assume that the reason for this is the desorption of the water with increasing temperature with its subsequent condensation in pores, which leads to a marked increase in the temperature ϵ' and ϵ'' of the sample. With the further increase in temperature, the evaporation of water occurs, and $\Delta\epsilon'(T)$ and $\epsilon''(T)$ decrease.

In Fig. 12, dependences of the increment of real part ($\Delta\epsilon' = \epsilon'(T) - \epsilon_{\infty}$, where $\epsilon_{\infty} = \epsilon'|_{T=-180^{\circ}\text{C}}$) of the dielectric permittivity on temperature on frequency 10 kHz are presented for investigated samples of MCC with different water contents.

It was shown in [16] that low-temperature relaxation process, which is connected with transition of methylol group from *tg* to *tt* conformation, can be described by the model with one relaxation time [17]

$$\tau = \frac{2\pi}{\omega} \frac{\exp(U/kT)}{1 + \exp(-V/kT)} \tag{8}$$

and for the increment of dielectric permittivity the following formula is valid:

$$\Delta\epsilon = \epsilon'(T) - \epsilon_{\infty} = \frac{N\mu^2}{3k\epsilon_0 T} \cdot \frac{\exp(-V/kT)}{[1 + \exp(-V/kT)]^2}, \tag{9}$$

where $\epsilon'(T)$ —is the dielectric permittivity of the sample at temperature T , N is the concentration of relaxation oscillators, μ^2 is the average square of difference of dipole moments of relaxation oscillators in two positions of equilibrium, and V is the difference of energies of relaxation oscillators in these equilibrium positions.

During approximation of the dependence of increment of real part of complex dielectric permittivity for MCC samples with different humidity by the dependence

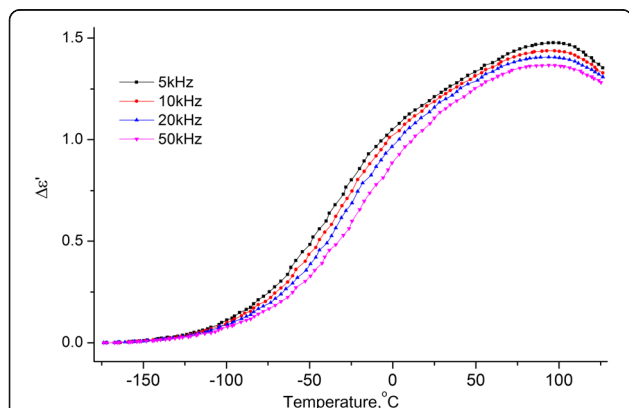


Fig. 10 Temperature dependence of the increment of real part of the dielectric permittivity MCC + 2.8% H₂O. Temperature dependence of the increment of real part ($\Delta\epsilon' = \epsilon'(T) - \epsilon_{\infty}$, where $\epsilon_{\infty} = \epsilon'|_{T=-180^{\circ}\text{C}}$) of the dielectric permittivity MCC + 2.8% H₂O on frequencies 5, 10, 20, and 50 kHz

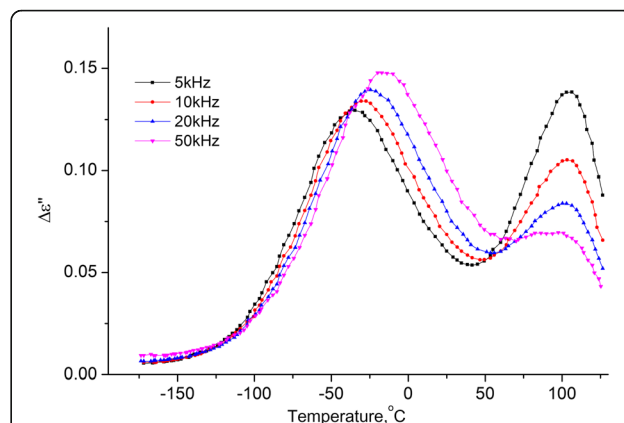


Fig. 11 Temperature dependence of imaginary part of the dielectric permittivity of MCC + 2.8% H₂O. Temperature dependence of imaginary part of the dielectric permittivity of MCC + 2.8% H₂O on frequencies 5, 10, 20, and 50 kHz

(Eq. 9), values of N and V were obtained (see Table 4) with regard for difference of dipole moments of relaxation oscillators in two equilibrium positions, which was calculated with regard for space structure of methylol group $\mu = 5.57D = 18.381 \cdot 10^{-30}\text{C} \cdot \text{m}$.

It is seen from Table 4 that at the growth of water content, energy difference V does not change, but concentration of methylol groups, which contributes in dielectric relaxation, increases.

In Fig. 13, dependences of imaginary part of dielectric permittivity on temperature on the frequency $f = 10$ kHz for studied samples of MCC with different water content are presented.

For relaxation process under approximation of one time of relaxation ($\tau = \tau_0 \exp((U - T\Delta S)/kT)$) and under

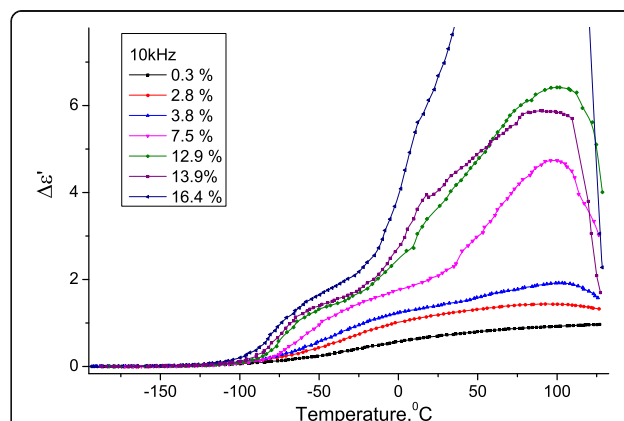


Fig. 12 Temperature dependence of the change of increment of the real part of the dielectric permittivity of MCC. Temperature dependence of the change of increment of the real part ($\Delta\epsilon' = \epsilon'(T) - \epsilon_{\infty}$, where $\epsilon_{\infty} = \epsilon'|_{T=-180^{\circ}\text{C}}$) of the dielectric permittivity of MCC samples with different water content

Table 4 Concentration of relaxation oscillators N and energies difference V for the samples of MCC with different water content

C (water content in MCC), %	0.3	2.8	3.8	7.5	12.9	13.9	16.4
V , kJ/mole	6.7	6.7	6.7	6.7	7	7	7.3
N , 10^{23} m^{-3}	40	65	76	117	139	150	213

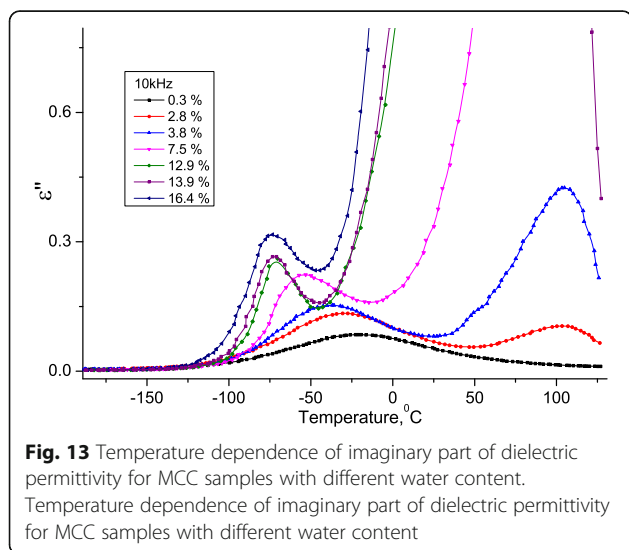
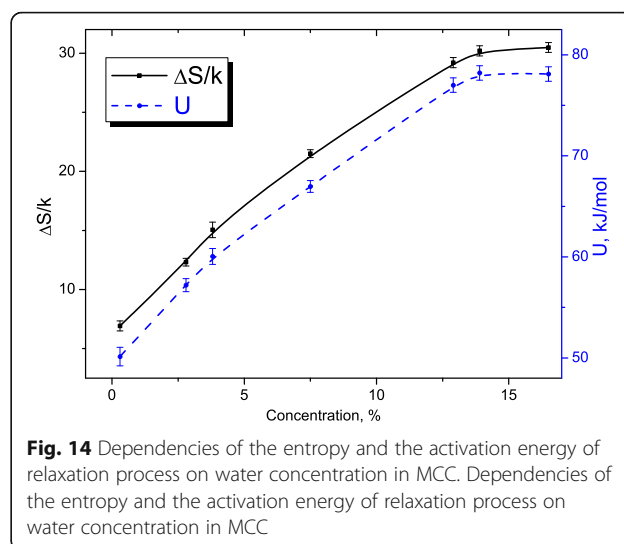
condition of maximum of dependence of the imaginary part of complex dielectric permittivity ($\epsilon''(T, f)$) $\omega\tau = 1$, changes of entropy $\Delta S/k$ (see Fig. 14) and activation energy U (see Fig. 14) with water concentration were obtained.

We assume that entropy of activation of the relaxation process is connected with the probability of formation of hydrogen bonds of methylol group with surrounding molecules of water [18].

Its growth testifies to the increase of the average number of water molecules, which surround these groups on the surface of MCC crystallites.

The saturation of the dependence $\Delta S/k$ (see Fig. 14) at growth of the water concentration is a consequence of formation of solid hydrate shell in the system of MCC crystallites as a result of incorporation of separate surface clusters from water molecules after reaching of their threshold concentration, which is determined by available water specific surface of MCC crystallites system during their swelling.

The growth of activation energy $U(C)$ of the relaxation process (see Fig. 14) and saturation of its dependence on water concentration has the same nature as for entropy activation is indicative of structuring of the surface of MCC crystallites during formation of their solid hydrate shell.

**Fig. 13** Temperature dependence of imaginary part of dielectric permittivity for MCC samples with different water content. Temperature dependence of imaginary part of dielectric permittivity for MCC samples with different water content**Fig. 14** Dependencies of the entropy and the activation energy of relaxation process on water concentration in MCC. Dependencies of the entropy and the activation energy of relaxation process on water concentration in MCC

Conclusions

Studies of dielectric, thermophysical, and structural properties of MCC samples with different degree of humidity were performed. The existence of relaxation process, which is connected with reorientation of the surface methylol groups of cellulose molecule by the change of their conformations from tg to tt is shown.

During the holding of the MCC sample in the saturated water vapor, the hydrate shell begins to form gradually on the surface of cellulose crystallites. It structures the boundary layer of MCC crystallites. At water concentration, higher than 13% formation of solid hydrate shell on MCC crystallites is observed.

Formation of hydrate shell results in the shift of relaxation process to the side of low temperatures due to its influence on the potential barrier and change of vibrations in equilibrium positions of surface methylol groups of the cellulose molecule at their transition from conformation tg to tt .

Acknowledgements

The authors thank the company Harke Group for providing MCC samples. The work objective was the investigation of the effect of water on the structure and dielectric relaxation of the microcrystalline cellulose.

Funding

This study was funded by the 14BF051-01 Taras Shevchenko National University of Kyiv.

Authors' Contributions

KK contributed to the preparation of the samples, research dielectric properties of the samples, and analysis of the results. OA designed the development of strategy of this work and its scientific management and analysis of the results. ML processed the experimental data and construction of models of physical processes. ST focused on the measurement thermogravimetric studies. YG researched X-ray diffraction experiments and analyzed the results. YZ participated in the analysis of the results and construction of models of physical processes. All authors read and approved the final manuscript.

Competing Interests

The authors declare that they have no competing interests.

Publisher's Note

Springer Nature remains neutral with regard to jurisdictional claims in published maps and institutional affiliations.

Received: 4 January 2017 Accepted: 12 July 2017

Published online: 26 July 2017

References

1. Mihranyan A, Llagostera AP, Karmhag R, Strømme M, Ek R (2004) Moisture sorption by cellulose powders of varying crystallinity/international. *J Pharm* 269(2):433–442
2. Azizi Samir MA, Alloin F, Dufresne A (2005) Review of recent research into cellulosic whiskers, their properties and their application in nanocomposite field. *Biomacromolecules* 6(2):612–626
3. Azizi Samir MAS, Alloin F, Gorecki W, Sanchez JY, Dufresne A (2004) Nanocomposite polymer electrolytes based on poly(oxyethylene) and cellulose nanocrystals. *J Phys Chem B* 108:10845–10852
4. Nedilko SG, Revo SL, Chornii VP, Scherbatskyi VP, Nediello MS (2015) Luminescent determination of nitrite traces in water solutions using cellulose as sorbent. *J Sens Sens Syst* 4:31–36
5. Karakawa M, Chikamatsu M, Nakamoto C, Maeda Y, Kubota S, Yase K (2007) Organic light-emitting diode application of fluorescent cellulose as a natural polymer. *Macromol Chem Phys* 208:2000–2006
6. Gelin K, Bodin A, Gatenholm P, Valizadeh S, Mihranyan A, Edwards K, Strømme M (2007) Characterization of water in bacterial cellulose using dielectric spectroscopy and electron microscopy. *Polymer* 48:7623–7631
7. Bras DL, Strømme M, Mihranyan A (2015) Characterization of dielectric properties of nanocellulose from wood and algae for electrical insulator applications. *J Phys Chem B* 119(18):5911–5917
8. Safari S, Theo G, Van De Ven M (2016) Effect of water vapor adsorption on electrical properties of carbon nanotube/nanocrystalline cellulose composites. *ACS Appl Mater Interfaces* 8(14):9483–9489
9. Kocherbitov V, Ulvenlund S, Kober M, Jarring K, Arnebrant T (2008) Hydration of microcrystalline cellulose and milled cellulose studied by sorption calorimetry. *J Phys Chem B* 112:3728–3734
10. Radugin MV, Lebedeva TN, Prusov AN, Zakharov AG (2010) Enthalpies of interaction of water with microcrystalline cellulose having different degrees of dispersion. *Russ J Phys Chem A* 84:1478–1480
11. Alekseev AN, Lazarenko MM, Lazarenko MV, Kovalev KN, Tkachev S. Yu Study of dielectric properties in region of liquid–solid phase transition// Industrial Laboratory. Materials Diagnostics. Vol.82. №. 9, 2016. P. 43–47
12. Pichkur V, Lazarenko M, Alekseev O, Kovbasa V, Lazarenko M (2015) Thermogravimetric research of the extruded and native types of starch. *Eastern-European Journal of Enterprise Technologies* 1(73):52–56
13. Prytulka N, Fedorova D, Lazarenko M, Vasylieva O, Yudina T (2016) The study of thermal processes in fish and plant semi-products / EUREKA: Life sciences 5:45–53. <http://dx.doi.org/10.21303/2504-5695.2016.00233>
14. Driemeier C, Calligaris GA (2011) Theoretical and experimental developments for accurate determination of crystallinity of cellulose I materials. *J Appl Cryst* 44:184–192. <https://doi.org/10.1107/S0021889810043955>
15. Leppänen K, Andersson S, Torkkeli M et al (2009) Structure of cellulose and microcrystalline cellulose from various wood species, cotton and flax studied by X-ray scattering. *Cellul* 16:999–1015
16. Nediello M, Hamamda S, Alekseev O, Chornii V, Dashevskii M, Lazarenko M, Kovalov K, Nedilko SG, Tkachov S, Revo S, Scherbatskyi V (2017) Mechanical, dielectric, and spectroscopic characteristics of “micro/nanocellulose+ oxide” composites. *Nanoscale Res Lett* 12:98. doi:10.1186/s11671-017-1862-x
17. John D, Hoffman G, Williams E (1966) Passaglia analysis of the α , β , and γ relaxations in polychlorotrifluoroethylene and polyethylene: dielectric and mechanical properties /. *J Polym Sci, Polym Symp* 11(1):173
18. Glasstone S, Laidler KJ, Eyring H (1941) The theory of rate processes: the kinetics of chemical reactions, viscosity, diffusion and electrochemical phenomena. McGraw-Hill, New York

Submit your manuscript to a SpringerOpen® journal and benefit from:

- Convenient online submission
- Rigorous peer review
- Open access: articles freely available online
- High visibility within the field
- Retaining the copyright to your article

Submit your next manuscript at ► springeropen.com